

Fiber-integrated cantilever-based nanomechanical biosensors as a tool for rapid antibiotic susceptibility testing

JIE ZHOU,^{1,2,†} JIABIN HUANG,^{1,2,†} HAOQIANG HUANG,^{1,2} CONG ZHAO,³ MENGQIANG ZOU,^{1,2} DEJUN LIU,^{1,2} XIAOYU WENG,¹  LIWEI LIU,¹ JUNLE QU,¹ LI LIU,⁴ CHANGRUI LIAO,^{1,2,*}  AND YIPING WANG^{1,2} 

¹Key Laboratory of Optoelectronic Devices and Systems of Ministry of Education and Guangdong Province, College of Physics and Optoelectronic Engineering, Shenzhen University, Shenzhen 518060, China

²Shenzhen Key Laboratory of Photonic Devices and Sensing Systems for Internet of Things, Guangdong and Hong Kong Joint Research Centre for Optical Fiber Sensors, Shenzhen University, Shenzhen 518060, China

³Laboratory of Artificial Intelligence and Digital Economy (SZ), Shenzhen, 518000, China

⁴Department of Electronic Engineering, Chinese University of Hong Kong, Hong Kong, China

[†]These authors contributed equally to this work.

*cliao@szu.edu.cn

Abstract: There is an urgent need for developing rapid and affordable antibiotic susceptibility testing (AST) technologies to inhibit the overuse of antibiotics. In this study, a novel microcantilever nanomechanical biosensor based on Fabry–Pérot interference demodulation was developed for AST. To construct the biosensor, a cantilever was integrated with the single mode fiber in order to form the Fabry–Pérot interferometer (FPI). After the attachment of bacteria on the cantilever, the fluctuations of cantilever caused by the bacterial movements were detected by monitoring the changes of resonance wavelength in the interference spectrum. We applied this methodology to *Escherichia coli* and *Staphylococcus aureus*, showing the amplitude of cantilever's fluctuations was positively related to the quantity of bacteria immobilized on the cantilever and associated with the bacterial metabolism. The response of bacteria to antibiotics was dependent on the types of bacteria, the types and concentrations of antibiotics. Moreover, the minimum inhibitory and bactericidal concentrations for *Escherichia coli* were obtained within 30 minutes, demonstrating the capacity of this method for rapid AST. Benefiting from the simplicity and portability of the optical fiber FPI-based nanomotion detection device, the developed nanomechanical biosensor in this study provides a promising technique for AST and a more rapid alternative for clinical laboratories.

© 2023 Optica Publishing Group under the terms of the [Optica Open Access Publishing Agreement](#)

1. Introduction

As a major invention in the history of human medicine, antibiotics have made great contributions to the human health in the past hundred years [1]. However, because of the worldwide abuse of antibiotics, the anti-microbial resistance (AMR) of antibiotics has become a major threat to global health [2]. Clinically, in order to deal with the complicated and serious bacterial infections or the cases in which broad-spectrum antibacterial drugs are ineffective, the antimicrobial susceptibility tests (AST) were carried out to find sensitive antimicrobial drugs, so as to achieve precise treatment [3,4]. However, most AST methods currently available in hospitals are based on bacterial culture methods, which are usually time-consuming, needing 24–48 hours, costly and labor intensive [5]. Therefore, it cannot be applied to the formulation of antibacterial prescriptions on large scale. In order to slow down the progress of antimicrobial resistance threat,

the development of rapid and affordable AST technologies has been a hot topic in the academical and clinical fields [6–8].

Over the last decades, many new approaches have emerged, such as flow cytometry [9], microfluidics [10], Raman spectroscopy [11], single-bacterium analysis [12,13], which improve the AST profile in the aspect of ease of operation, economy, and low experimental duration. Moreover, biosensors are increasingly a preferred choice for developing AST point-of-care platforms owing to its advantages of simplicity, robustness, label-free, and real-time analysis [14]. The microcantilever-based nanomechanical biosensor is extremely sensitive to the molecules adsorbed on the surface of microcantilever, which could convert the biochemical processes in situ into mechanical signals, so as to realize the monitoring of biochemical reactions, the quantitative or qualitative detection of molecules [15,16]. As a label-free, rapid and real-time sensing method, the nanomechanical biosensors have been extensively applied in the healthcare [17,18], cell analysis [19,20], and environmental monitoring [21,22]. In 2013, Longo and coworkers immobilized bacteria on the microcantilever beam of a nanomechanical sensor and assessed the metabolic activity of bacteria (*Escherichia coli* and *Staphylococcus aureus*) in the presence of antibiotics (ampicillin and kanamycin) by monitoring the fluctuations of microcantilever, creating a precedent for nanomechanical sensors to be used in rapid AST [23]. Later, this detection scheme was successfully tested with various antimicrobial compounds [20,24], many different organisms [25–27], and in detection of actual samples [28], making it a promising technology in the field of AST [29].

Typically, the optical lever technique was utilized for the precise readout of the microcantilever fluctuation in AST, which is similar to that used in an atomic force microscopy (AFM) readout [19,23–25,27–30]. However, the optical lever technique still has some weakness when it is used in practical AST. Firstly, in order to realize accurate optical lever amplification, the sensing part should be separated far from the light source and the collection device, making the detection device to be bulky, cumbersome and expensive, which is disadvantageous for practical AST, especially in the primary health care institutions. Furthermore, the external ambient noise would greatly affect the accuracy of sensors because of the serious loss of optical signal by the use of spatial light transmission and collection [31]. Thus, it is essential to develop a new demodulation technique for the readout of microcantilever's fluctuations to achieve portable AST detection.

In this paper, for the first time, we integrate the single mode fiber (SMF) and the microcantilever together to develop a nanomechanical biosensor based on Fabry–Pérot interference demodulation for AST. The optical interference readout can realize not only miniaturized nanomechanical sensors but also low transmission losses by utilizing the fiber as the medium of light transmission and collection [32]. The developed biosensor was fabricated by assembling a commercial microcantilever probe right above a SMF's end face. And the tip of the microcantilever was aligned with the core of the SMF (Fig. 1). In this way, an Fabry–Pérot interferometer (FPI) was generated between the optical-fiber end face and the cantilever. Combining the advantages of low K value of the commercial cantilever and high sensitivity of the optical interference readout, the weak fluctuations of cantilevers induced by the movements of bacteria immobilized on the cantilever can be transformed into the change of the cavity length of the FPI, which can be traced by monitoring the shift of dip wavelength observed in the interference spectrum. The utility of the method was demonstrated by measuring the antimicrobial susceptibility of *Escherichia coli* (*E. coli*) and *Staphylococcus aureus* (*S. aureus*) to three categories of antibiotics: ampicillin, ceftriaxone and ciprofloxacin, and obtaining the minimum inhibitory and bactericidal concentrations (MIC/MBC) of ampicillin for *E. coli* within 30 min.

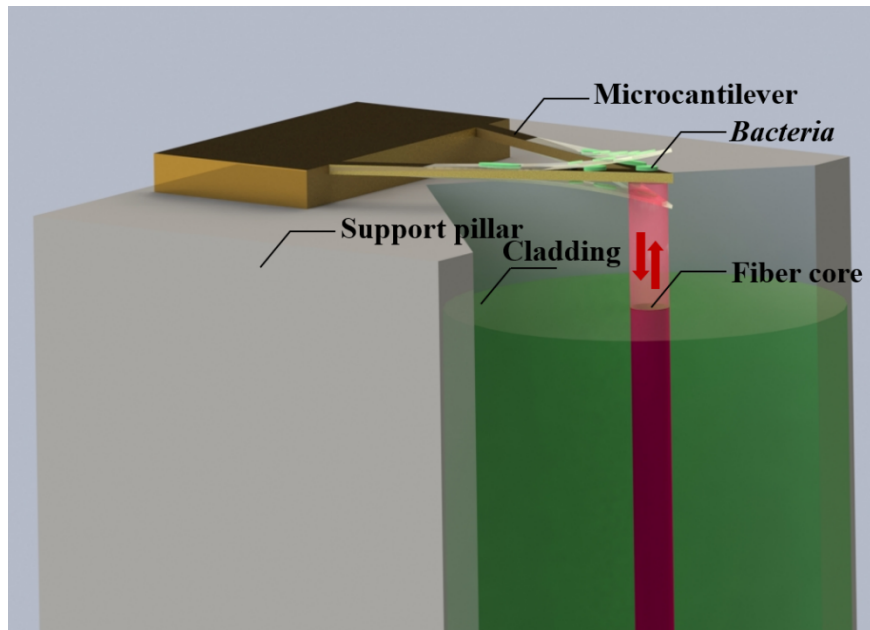


Fig. 1. Schematic diagram of the nanomechanical sensor based on a cantilever integrated on the fiber end face.

2. Material and methods

2.1. Chemicals

The phosphate buffered saline (PBS, 0.01 M, pH = 7.4), concentrated sulfuric acid, hydrogen peroxide (30%), glucose, NaCl, peptone, yeast powder and glutaraldehyde were supplied by Aladdin Co., Ltd. (Shanghai, China). The antibiotics, ampicillin sodium, ceftriaxone sodium and ciprofloxacin hydrochloride, all with analytical grade, were obtained from Topscience Co., Ltd. (Shanghai, China). The freeze-dried powder of *E. coli* (CMCC44103) and *S. aureus* (ATCC29213) was brought from BNCC (China).

The lysogeny broth (LB) culture medium was prepared as follows: Firstly, take 10 g of peptone, 5 g of yeast powder and 10 g of NaCl in a 1 L beaker, then add deionized water in the beaker to about 1 L. The mixture was stirred evenly while heating. Next, the pH of the medium was adjusted to 7.2 with standard NaOH solution (1 M). Finally, the prepared solution was put into a triangular flyer for autoclaving.

Ampicillin is an antibiotic of the penicillin class, which can inhibit the synthesis of bacterial cell wall through the binding of β -lactam ring to the drug receptor-penicillin-binding protein in bacteria, and then activate the role of autolysin in bacterial cell wall to dissolve the bacteria, resulting in the death of the microorganisms. Ceftriaxone is a cephalosporin antibiotic that has a similar mechanism of penicillin and a broader antibacterial spectrum than ampicillin. Ciprofloxacin is a quinolone antibiotic that acts as a bactericidal agent by inhibiting bacterial DNA synthesis.

2.2. Fabrication of nanomechanical biosensor and experimental setup

Figure 2(A) shows the experimental setup of the developed nanomechanical biosensor. The incident light emitted by the broadband light source (BBS, FL-ASE-EB-D-2-3-FC, FiberLake) travelled through the 3 dB coupler and reached the sensor, then the reflected light of the sensing

module passed through the 3 dB coupler and was finally received by a near-infrared spectrometer (NIRQuest512, Ocean optics). The reflection spectrums were analyzed using MATLAB. The “spline interpolation” and “polynomial fitting” algorithms were used to fit the reflection spectrum for addressing the resonance dip wavelength.

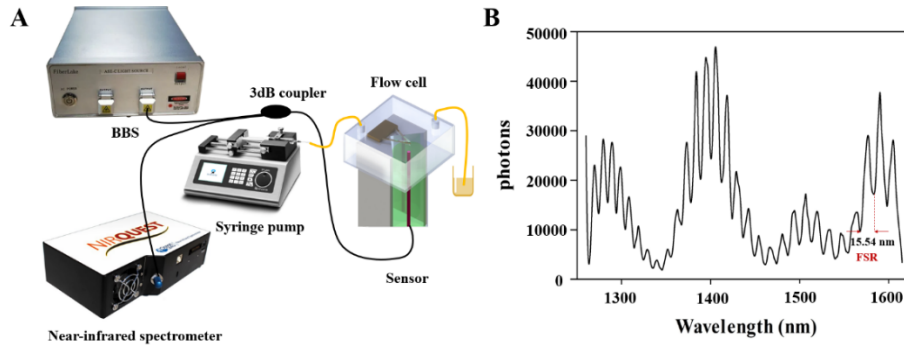


Fig. 2. (A) Experimental setup of the developed nanomechanical biosensor. (B) The measured reflection spectrum of the sensor at 1260-1615 nm.

We used a commercial triangular cantilever (NP-O10, Bruker, $k=0.06$) as the sensing unit, which was treated with glutaraldehyde to provide a compatible interface for bacteria immobilization. Specifically, the cantilever was firstly cleaned with the piranha solution (concentrated sulfuric acid: 30% hydrogen peroxide = 3:1) for 15 minutes, rinsed thoroughly with deionized water, and dried in air. Then the cantilever was immersed in the 1% glutaraldehyde solution for 15 min, rinsed thoroughly with deionized water, and dried in air. The bacteria could be attached to glutaraldehyde-functionalized surface by the reaction of amino groups on the proteins of bacterial cell wall [33].

The nanomechanical biosensor was fabricated by assembling the chemically treated cantilever with a SMF (Fig. 1). The 1550 nm SMF (YOFC) was chosen to use in the experiment because its low cost and accessibility. Firstly, the SMF, pre-cut by a fiber cutter to produce a flat end face, was packaged at the groove of a customized resin column (support pillar) to keep it upright, and then the cantilever was fixed on the upper surface of the column. During the fabrication process, the reflected light of the sensing module was received by an optical spectrum analyzer (OSA). The tip center of the cantilever was made to align with the core of SMF under the microscope and the offset should not be more than 10 μm , thus forming an FPI. The cavity length of FPI is a vital factor for the performance of FPI. To obtain the high-contrast interference spectrum while improving the sensitivity of the sensor, the cavity length is controlled at 50-100 μm , which can be calculated according to Eq (1) [33].

$$FSR = |\lambda_{m+1} - \lambda_m| = \frac{\lambda_{m+1}\lambda_m}{2nL} \quad (1)$$

Where n is the refractive index of air in the cavity ($n = 1$). The free spectral range (FSR) is the difference of resonance wavelengths between two adjacent interference levels (λ_m and λ_{m+1}) in the interference spectrum for the sensor in air. As a result, the interference contrast of the reflection spectrum should be at least 6 dB, and the FSR at 1550 nm is between 12-25 nm. Finally, the SMF and the probe were reinforced with the ultraviolet curing adhesive to avoid displacement. During the bacteria experiments, the sensor was fixed in a flow cell with a volume of 200 μL . The liquids were injected into the flow cell by a syringe pump (LSPO21B, Longer) in a flow rate of 100 $\mu\text{L}/\text{min}$. It should be noted that all measurements are taken at least one minute after the pump is shut down. The sensor with the flow cell was placed in a homemade shielding box to

isolate it from the interference of external environment. The flow cell and resin column were drawn with Solidworks and printed with a 3D printer (Form3, FormLabs). All experiments in this work were conducted at ambient temperature (23 °C-27 °C).

2.3. Preparation of *E. coli* and *S. aureus*

E. coli is a typical Gram-negative short bacilli and 0.5× 1-3 microns in size. It is a resident flora in the intestines of humans and animals and can cause extra-intestinal infection under certain conditions. *Staphylococcus aureus* (*S. aureus*), belongs to the genus *Staphylococcus*, is a representative of Gram-positive bacteria, and is a common foodborne pathogenic microorganism. The typical *S. aureus* was spherical, about 0.8µm in diameter, and arranged into grape clusters under the microscope.

Frozen stocks of *E. coli* or *S. aureus* were stored at -80°C in glycerol-supplemented LB. The frozen *bacteria* were thawed in the clean bench, and a small amount of bacterial liquid was dipped into the inoculation ring and streak inoculated on the surface of a LB agar plate. The LB agar plate was then placed in the bacterial incubator for overnight culture at 37°C. A single bacterial colony was selected and transferred into a tube containing LB medium by an inoculation ring. Then the tube was placed in a shaker and shaken overnight at 37°C under 180 rpm of shaking speed. The cultured bacterial solution was washed and resuspended with PBS or LB for subsequent experiments. The concentration of *bacteria* determined by an ultraviolet spectrophotometer (UV-8000, METASH). In our experiments, we adjust the *E. coli* suspensions to 1×10^9 CFU/mL by a OD₆₇₀ of ~0.3.

2.4. Antibiotic susceptibility test

For assessing the bacterial response to the exposure of antibiotics, firstly, the LB solution was injected into the flow cell. The fluctuations of the sensor in blank LB were measured for 5 min (labelled 'LB'). Then the LB solution containing living *E. coli* or *S. aureus* was injected into the flow cell and left to incubate for 30 min to ensure the attachment of bacteria. Next, the LB solution was flowed into the flow cell to wash away loosely adhering or floating bacteria. The fluctuations of the sensor after bacteria attachment were collected for 5 min and labelled 'Bacteria in LB'. Lastly, the LB solution containing antibiotics with determined concentration was injected into the flow cell and left to take effect for 30 min. The fluctuations of the sensor after antibiotic treatment were recorded for 5 min, and were labelled after the chosen antibiotic. For *E. coli*, the tested concentration for ceftriaxone and ciprofloxacin was set as 10 µg/ml. And the tested concentration for ampicillin was set as 5µg/ml, 10 µg/ml, 20µg/ml, 50 µg/ml and 100 µg/ml in order to obtain the MIC and MBC for *E. coli*. For *S. aureus*, the tested concentration for ampicillin was set as 10 µg/ml.

2.5. Exposure of *E. coli* to glucose

To study the effect of glucose to the *E. coli*, after the bacteria had attached on the cantilever, the PBS solution was injected into the chamber and left to stabilize for about 1 h. Then the fluctuation signal of the sensor was collected for 5 min. After that, 2.5% glucose or 5% glucose was injected into the chamber and left to stabilize for about 20 min. The fluctuation signal of the sensor was recorded for 5 min and labelled as "2.5% glucose" and "5% glucose".

3. Results and discussions

3.1. Theoretical Basis

The reflection spectrum was measured using a BBS with a near-infrared spectroscopy, as shown in Fig. 2(B). The reflection spectrum was formed by the interference of two light beams in SMF, i.e., the light reflected at the fiber end face and the light reflected at the lower surface of the

cantilever, respectively. Consequently, an FPI was formed by an air microcavity between the fiber end face and the lower surface of the microcantilever, which was chosen for demodulation since the cavity length of the FPI was changed with the fluctuations of cantilever, leading to a change of dip wavelength in the reflection spectrum of SMF. The relationship between the dip wavelength shift ($\Delta\lambda_r$) and the cavity length shift (ΔL) is represented as $\Delta\lambda_r/\lambda_r = \Delta L/L$, where, λ_r is the dip wavelength, and L is the cavity length of the FPI. Thus, the cantilever's fluctuations can be calculated by tracing the changes in dip wavelength of a specific resonance peak in the reflection spectrum.

3.2. Optimization of the incubating concentration of *E. coli*

The incubating concentration of bacteria determines the number of bacteria immobilized on the cantilever and is important for detecting bacterial movements. Thus, the incubating concentration of *E. coli* needs to be optimized before experiments. Figure 3(D)-(G) shows the fluctuations of sensors under the condition of PBS (without bacteria), incubating concentration of 1×10^8 CFU/mL, 3×10^8 CFU/mL and 1×10^9 CFU/mL *E. coli*. It should be noted that the fluctuations of sensors were all measured in PBS. It can be seen that when the sensor was stabilized in blank PBS, the deflection of cantilever was slight and smooth (Fig. 3(D)), with a small deflection variance of 0.07 nm^2 (Fig. 3 H). After the *E. coli* had been immobilized on the cantilever, the fluctuations of sensors became obvious and random with sparse peaks (1×10^8 CFU/mL and 3×10^8 CFU/mL) or dense peaks (1×10^9 CFU/mL), which indicated the movements of bacteria on the cantilever. The magnitude of fluctuations was positively related on the incubating concentration of bacteria, which could also be illustrated by the variance of fluctuations. At the end of selected experiments, the used cantilevers were firmly attached to the sample stage, gold sprayed with an ion sputtering apparatus (SBC-12, KYKY) for 5 min, and imaged in a scanning electron microscope (Phenom pro, Phenom-world BV). The SEM images in Fig. 3(A)-(C) and Fig. S1 represents the images of attached *E. coli* on the cantilever under the incubating concentration of 1×10^8 CFU/mL, 3×10^8 CFU/mL and 1×10^9 CFU/mL. When the incubation concentration of *E. coli* was set to be 1×10^8 CFU/mL, only a few bacteria were successfully immobilized on the cantilever. When the incubation concentration of *E. coli* was increased to 3×10^8 CFU/mL, more bacteria could be seen on the cantilever (about one hundred). And a significant increase in the bacteria quantity (several hundreds) on the cantilever was observed when the incubation concentration of *E. coli* was set as 1×10^9 CFU/mL. The above results demonstrated that the overall fluctuations of cantilever were positively related to the quantity of bacteria immobilized on the cantilever. Since we expect that the variance of fluctuations after the attachment of bacteria could be enhanced by at least 10 time compared with that of the blank PBS group, the incubation concentration of *E. coli* was chosen to be 1×10^9 CFU/mL.

3.3. Monitoring of bacterial response under the stimulus of glucose

To better explain the relationship between bacterial movements and cantilever's fluctuations, we investigated the response of *E. coli* to different concentrations of glucose (2.5% and 5%). The glucose could activate the metabolic cycle of bacteria. As shown in the Fig. 4, the fluctuations of cantilever were increased when the bacteria were exposed to glucose compared to the PBS control group. The variance of deflection was increased by 0.43 and 1.29 times for the bacteria in 2.5% glucose and 5% glucose, respectively. The dependence of deflection variance on the glucose concentration indicated that the deflections were produced by an active metabolic process of bacteria, not by Brownian motion [23,34].

3.4. Antibiotic Susceptibility Test

We measured the fluctuations of cantilever under the conditions of blank nourishing medium (LB), bacteria attachment on the cantilever, and 30 minutes of treatments with $10 \mu\text{g/ml}$ of

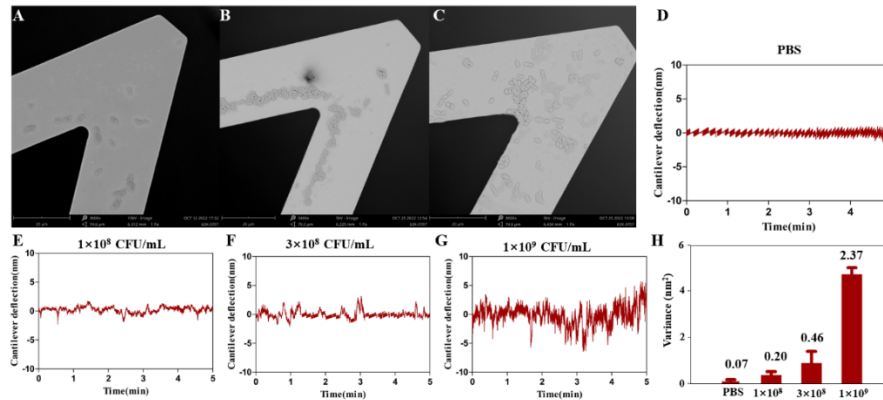


Fig. 3. (A-C) The SEM images of the tip of the cantilevers taken at the end of each experiment when the incubating concentration of *E. coli* was set as 1×10^8 CFU/mL (A), 3×10^8 CFU/mL (B) and 1×10^9 CFU/mL (C); (D) The deflection curves of cantilevers in blank PBS; (E-G) The deflection curves of cantilevers for *E. coli* in PBS when the incubating concentration of *E. coli* was set as 1×10^8 CFU/mL (E), 3×10^8 CFU/mL (F) and 1×10^9 CFU/mL (G). The deflection of each cantilever was recorded for 5 min. (H) The variance value of the deflection curves under the above conditions. The mean value and error bars are calculated by statistical results of the three measurements in the similar conditions.

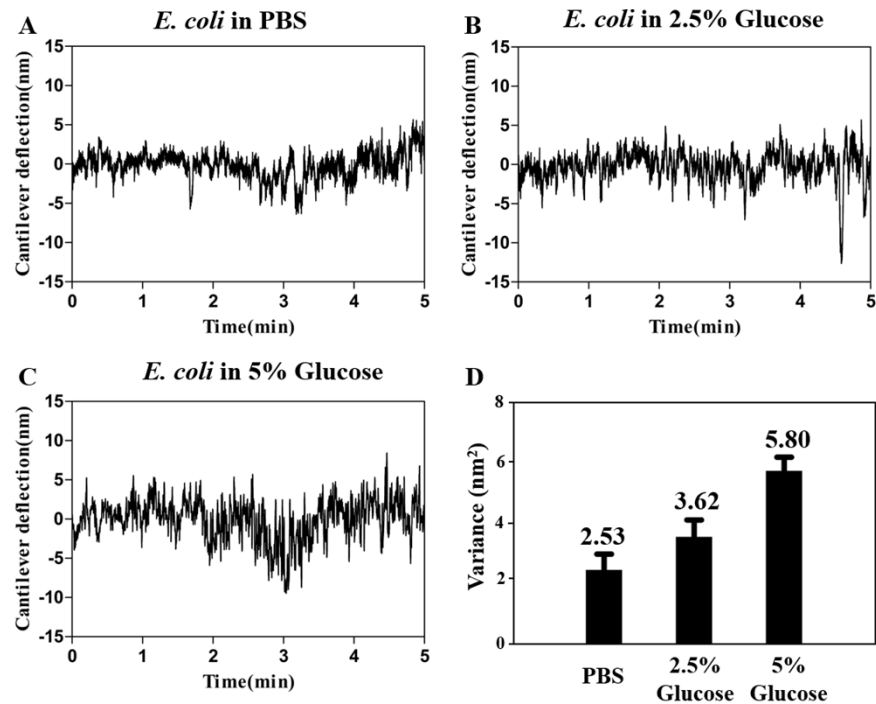


Fig. 4. Experiments describing the response of *E. coli* to glucose. (A-C) The deflection curves of cantilevers for *E. coli* in PBS (A), in 2.5% glucose (B) and in 5% glucose (C). The deflection of each cantilever was recorded for 5 min. (D) The variance value of the deflection curves under the above conditions. The mean value and error bars are calculated by statistical results of the three measurements in the similar conditions.

antibiotics, i.e., ciprofloxacin, ceftriaxone and ampicillin prepared in LB. As shown in Fig. 5, the cantilevers exhibited very mild fluctuations in the blank LB, which were similar with that in blank PBS. After the attachment of *E. coli*, the cantilever's fluctuations greatly increased. Moreover, the variance of deflection when the attached bacteria were nourished in LB was larger than those in PBS, which was attributed to that the LB promoted the metabolism of the bacteria, reinforcing the point that the cantilever's fluctuations were strongly dependent on the metabolism activity of bacteria. After the *E. coli* were incubated with antibiotics for 30 min, the fluctuations of cantilevers decreased sharply for ceftriaxone and ciprofloxacin, and slightly for ampicillin at the same concentration (10 $\mu\text{g/ml}$). The variance of cantilevers' deflections dropped to 26.4%, 37.6% and 75.2% of its original value for ciprofloxacin, ceftriaxone and ampicillin, respectively, demonstrating that the fluctuations of cantilevers could be used to assess the motility of bacteria and associated changes in response to antibiotics treatment. It can be concluded that the order of antibiotic susceptibility for the *E. coli* is as follows: ciprofloxacin > ceftriaxone > ampicillin. The antibiotic susceptibility for the *S. aureus* to ampicillin was also tested by treating *S. aureus* with 10 $\mu\text{g/ml}$ ampicillin. It was shown in Fig. 5(D) and Fig. 5 H that the ampicillin had induced a dramatic decrease in the metabolic activity of *S. aureus*. The variance of cantilevers' deflections dropped to 7.6% of its original value for ampicillin, which meant the *S. aureus* was much more sensitive to ampicillin than the *E. coli*.

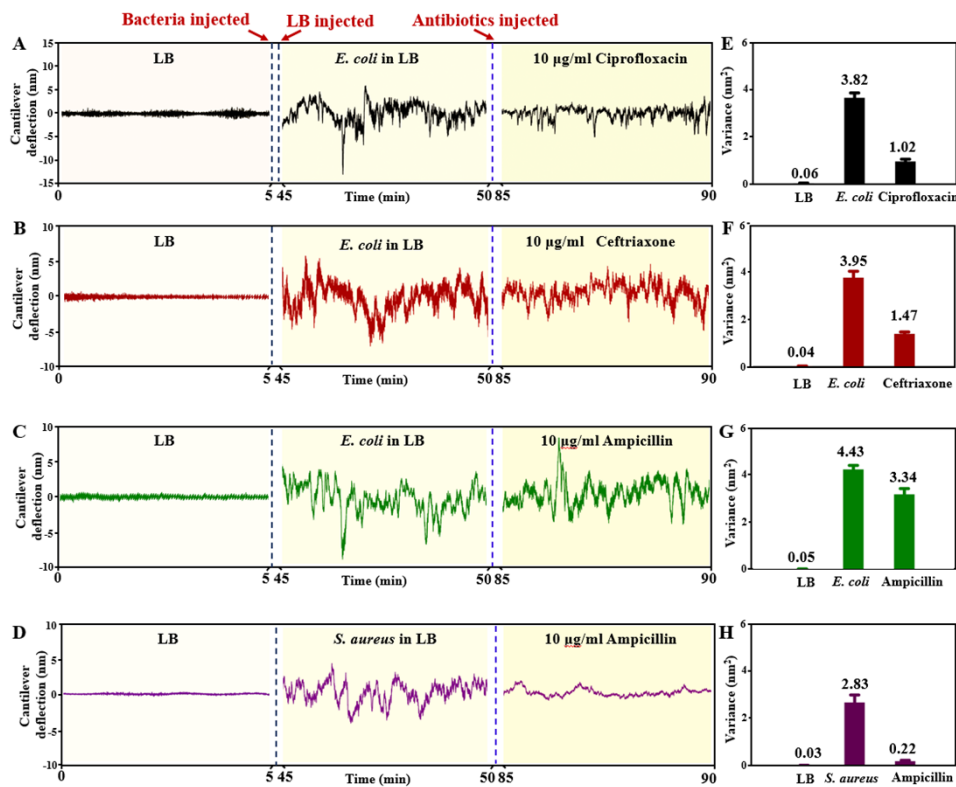


Fig. 5. Experiments describing the response of bacteria to different kinds of antibiotics. (A-C) The deflection curves of cantilevers for blank LB, *E. coli* in LB, and in 10 $\mu\text{g/ml}$ Ciprofloxacin (A), Ceftriaxone (B) and Ampicillin (C). The deflection of each cantilever was recorded for 5 min. (D) The deflection curves of cantilevers for blank LB, *S. aureus* in LB, and in 10 $\mu\text{g/ml}$ Ampicillin. (E-H) The variance value of the deflection curves under the above conditions. The mean value and error bars are calculated by statistical results of the three measurements in the similar conditions.

In order to verify the capability of this technique for quantitative antibiotic susceptibility test, we measured the *E. coli*'s response to different concentrations of ampicillin (5 µg/ml, 10 µg/ml, 20 µg/ml, 50 µg/ml and 100 µg/ml) prepared in LB. The fluctuations of cantilevers were recorded for 5 min after 30 minutes of exposure to the ampicillin. As represented in Fig. 6, there were inconspicuous changes in the fluctuations for 5 µg/ml and 10 µg/ml ampicillin compared with the “*E. coli* in LB” group. When the ampicillin concentration increased to 20 µg/ml, a noticeable decrease in the fluctuations could be seen. The fluctuations almost disappeared for 50 µg/ml and 100 µg/ml ampicillin, suggesting the death of *E. coli*. The normalized variance values for each ampicillin concentration were presented in Fig. 6 H and Table S1, suggesting that the nanomotion of bacteria were attenuated with the increasing concentration of ampicillin. And the relationship of normalized variance (NV) with ampicillin concentration was fitted using a sigmoid function [18] and presented as Eq. (2).

$$NV(C) = 0.077 + \frac{1.041}{1 + 10^{(15.05-C) \times (-0.068)}} \quad (2)$$

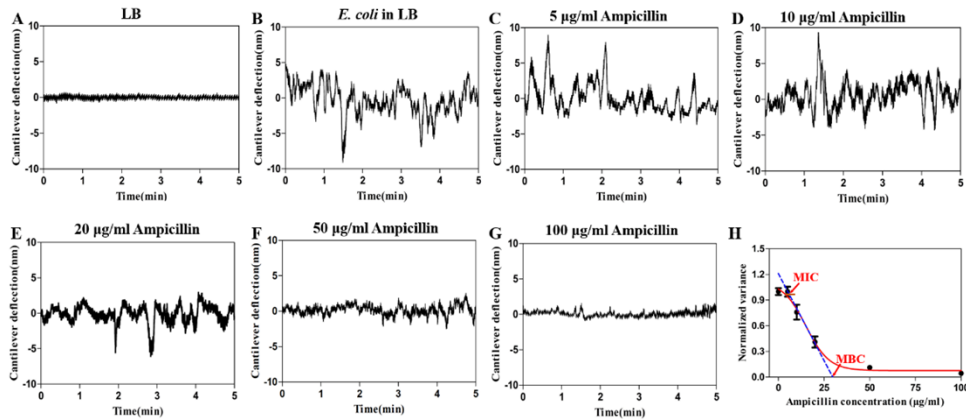


Fig. 6. Experiments describing the response of bacteria to different concentrations of ampicillin. (A-G) The deflection curves of cantilevers for blank LB (A), *E. coli* in LB (B), and in 5 µg/ml (C), 10 µg/ml (D), 20 µg/ml (E), 50 µg/ml (F), 100 µg/ml (G) Ampicillin. The deflection of each cantilever was recorded for 5 min. (H) The sigmoid fitting of the normalized variance with the ampicillin concentration (red curve). The normalized variance values were calculated by dividing the deflection variance of ampicillin group by the deflection variance of “*E. coli* in LB” group. The MIC and MBC values were obtained by intercepting the tangent of the fitted sigmoid curve at its inflection point (dashed blue line) with the 1 and 0 horizontal lines. The mean value and error bars are calculated by statistical results of the three measurements in the similar conditions.

The MIC and MBC are typically used to appraise the ability of antibiotics to resist pathogenic microorganisms. MIC refers to the lowest concentration of an antibiotic that can inhibit the growth of a bacterial strain in the medium, while MBC is defined as the lowest concentration of an antibiotic that kills most bacteria in the culture medium. For determining the value of MIC and MBC, a tangent line of the fitted sigmoid curve at its inflection point ($\log EC_{50} = 15.05$) was firstly obtained (dashed line in Fig. 6 H, $y = -0.0407 \times c + 1.21$), then the abscissas of intersection points of the tangent line with the horizontal lines $NV(C_{MIC}) = 1$ and $NV(C_{MBC}) = 0$ were calculated to be $C_{MIC} = 5.16$ µg/ml and $C_{MBC} = 29.72$ µg/ml. The above results had verified the capacity of the developed biosensor for rapid AST.

The frequency components of the fluctuations are also important indexes for characterizing the movements of bacteria. Figure 7 showed the power spectrum of the fluctuation curve for LB, *E.*

coli in LB, and 100 $\mu\text{g/ml}$ of ampicillin. It could be seen from Fig. 7(A) that the power spectrum for LB was relatively uniform without prominent frequency components. While for *E. coli* in LB, although there was still no distinct oscillatory component, the low frequency components (0-0.5 Hz) obviously accounted for a large proportion (52%) in the power spectrum (Fig. 7(B)). When the *E. coli* were treated with 100 $\mu\text{g/ml}$ ampicillin, the proportion of low-frequency components to the power spectrum declined sharply (25%), which indicated that the movements of *E. coli* were reduced by the ampicillin (Fig. 7(C)).

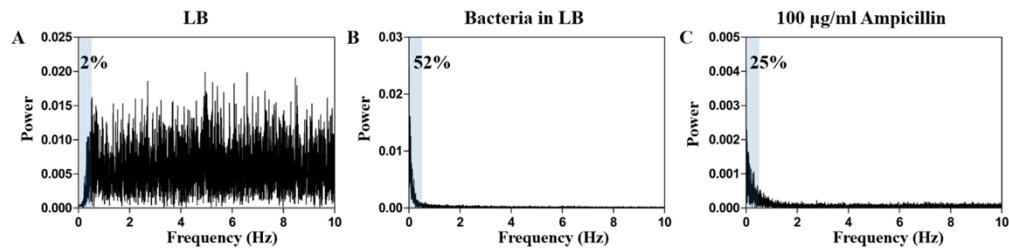


Fig. 7. The power spectrum of the fluctuation curve for LB (A), *E. coli* in LB (B), and 100 $\mu\text{g/ml}$ of ampicillin (C). The low frequency components (0-0.5 Hz) were labelled in blue color. And the percentage numbers indicated the power proportion of low frequency components (0-0.5 Hz) in the whole power spectrum.

4. Conclusions

This paper, for the first time, presents a miniature FPI-based microcantilever nanomechanical biosensor, in which a microcantilever is mounted parallelly to the fiber end face, as a label-free, sensitive and efficient analytical approach for antibiotic susceptibility testing. It allows us to detect the bacterial movements by monitoring the deflections of cantilever in a real time manner. We have proven its capabilities by studying the dynamic effects of different antibiotics on *E. coli*, establishing the quantitative standard for AST, i.e., MIC and MBC determination, for ampicillin within 30 minutes. Compared with the optic lever magnifying, the developed sensor provides a compact and simplified optical fiber-based demodulation system for AST, which has a broad prospect for clinical application.

Funding. National Natural Science Foundation of China (62122057, 62075136, 62205222, 62205221, 62105217); Science and Technology Innovation Commission of Shenzhen (RCYX20200714114524139, JCYJ20200109114001806, JCYJ20190808173401660).

Acknowledgments. This work was supported by National Natural Science Foundation of China (NSFC) (62122057, 62075136, 62205222, 62205221, 62105217); Science and Technology Innovation Commission of Shenzhen (RCYX20200714114524139, JCYJ20200109114001806, JCYJ20190808173401660).

Disclosures. The authors declare no conflicts of interest.

Data availability. Data underlying the results presented in this paper are not publicly available at this time but may be obtained from the authors upon reasonable request.

Supplemental document. See [Supplement 1](#) for supporting content.

References

1. K. Lewis, "The science of antibiotic discovery," *Cell* **181**(1), 29–45 (2020).
2. B. Aslam, W. Wang, M. I. Arshad, M. Khurshid, S. Muzammil, M. H. Rasool, M. A. Nisar, R. F. Alvi, M. A. Aslam, M. U. Qamar, M. K. F. Salamat, and Z. Baloch, "Antibiotic resistance: a rundown of a global crisis," *Infect. Drug Resist.* **11**, 1645–1658 (2018).
3. Z. A. Khan, M. F. Siddiqui, and S. Park, "Current and emerging methods of antibiotic susceptibility testing," *Diagnostics* **9**(2), 49 (2019).
4. K. Syal, M. N. Mo, H. Yu, R. Iriya, W. W. Jing, G. Sui, S. P. Wang, T. E. Grys, S. E. Haydel, and N. J. Tao, "Current and emerging techniques for antibiotic susceptibility tests," *Theranostics* **7**(7), 1795–1805 (2017).

5. D. C. Spencer, T. F. Paton, K. T. Mulroney, T. J. J. Inglis, J. M. Sutton, and H. Morgan, "A fast impedance-based antimicrobial susceptibility test," *Nat. Commun.* **11**(1), 5328 (2020).
6. N. Jo, B. Kim, S. M. Lee, J. Oh, I. H. Park, K. J. Lim, J. S. Shin, and K. H. Yoo, "Aptamer-functionalized capacitance sensors for real-time monitoring of bacterial growth and antibiotic susceptibility," *Biosens. Bioelectron.* **102**, 164–170 (2018).
7. M. Safavieh, H. J. Pandya, M. Venkataraman, P. Thirumalaraju, M. K. Kanakasabapathy, A. Singh, D. Prabhakar, M. K. Chug, and H. Shafiee, "Rapid real-time antimicrobial susceptibility testing with electrical sensing on plastic microchips with printed electrodes," *ACS Appl. Mater. Interfaces* **9**(14), 12832–12840 (2017).
8. P. Sabhachandani, S. Sarkar, P. C. Zucchi, B. A. Whitfield, J. E. Kirby, E. B. Hirsch, and T. Konry, "Integrated microfluidic platform for rapid antimicrobial susceptibility testing and bacterial growth analysis using bead-based biosensor via fluorescence imaging," *Microchim. Acta* **184**(12), 4619–4628 (2017).
9. F. David, M. Hebeisen, G. Schade, E. Franco-Lara, and M. Di Bernardino, "Viability and membrane potential analysis of *Bacillus megaterium* cells by impedance flow cytometry," *Biotechnol. Bioeng.* **109**(2), 483–492 (2012).
10. J. Dai, M. Hamon, and S. Jambovane, "Microfluidics for antibiotic susceptibility and toxicity testing," *Bioengineering* **3**(4), 25 (2016).
11. D. D. Galvan and Q. M. Yu, "Surface-enhanced Raman scattering for rapid detection and characterization of antibiotic-resistant bacteria," *Adv. Healthcare Mater.* **7**, 1701335 (2018).
12. D. Conteduca, G. Brunetti, F. Dell'Olio, M. N. Armenise, T. F. Krauss, and C. Ciminelli, "Monitoring of individual bacteria using electro-photonic traps," *Biomed. Opt. Express* **10**(7), 3463–3471 (2019).
13. M. Tardif, J. B. Jager, P. R. Marcoux, K. Uchiyamada, E. Picard, E. Hadji, and D. Peyrade, "Single-cell bacterium identification with a SOI optical microcavity," *Appl. Phys. Lett.* **109**(13), 133510 (2016).
14. B. Behera, A. G. K. Vishnu, S. Chatterjee, V. S. N. V. Sitaramgupta, N. Sreekumar, A. Nagabhusan, N. Rajendran, B. H. Prathik, and H. J. Pandya, "Emerging technologies for antibiotic susceptibility testing," *Biosens. Bioelectron.* **142**, 111552 (2019).
15. J. Tamayo, P. M. Kosaka, J. J. Ruz, Á San Paulo, and M. Calleja, "Biosensors based on nanomechanical systems," *Chem. Soc. Rev.* **42**(3), 1287–1311 (2013).
16. J. L. Arlett, E. B. Myers, and M. L. Roukes, "Comparative advantages of mechanical biosensors," *Nat. Nanotechnol.* **6**(4), 203–215 (2011).
17. P. Nautiyal, F. Alam, K. Balani, and A. Agarwal, "The role of nanomechanics in healthcare," *Adv. Healthcare Mater.* **7**(3), 1700793 (2018).
18. R. Mathew and A. Ravi Sankar, "A review on surface stress-based miniaturized piezoresistive SU-8 polymeric cantilever sensors," *Nano-Micro Lett.* **10**(2), 35 (2018).
19. X. Hang, S. He, Z. Dong, G. Minnick, J. Rosenbohm, Z. Chen, R. Yang, and L. Chang, "Nanosensors for single cell mechanical interrogation," *Biosens. Bioelectron.* **179**, 113086 (2021).
20. A. C. Kohler, L. Venturelli, G. Longo, G. Dietler, and S. Kasas, "Nanomotio detection based on atomic force microscopy cantilevers," *Cell Surf.* **5**, 100021 (2019).
21. P. S. Waggoner and H. G. Craighead, "Micro- and nanomechanical sensors for environmental, chemical, and biological detection," *Lab Chip* **7**(10), 1238–1255 (2007).
22. K. M. Goeders, J. S. Colton, and L. A. Bottomley, "Microcantilevers: sensing chemical interactions via mechanical motion," *Chem. Rev.* **108**(2), 522–542 (2008).
23. G. Longo, L. Alonso-Sarduy, L. M. Rio, A. Bizzini, A. Trampuz, J. Notz, G. Dietler, and S. Kasas, "Rapid detection of bacterial resistance to antibiotics using AFM cantilevers as nanomechanical sensors," *Nat. Nanotechnol.* **8**(7), 522–526 (2013).
24. I. Bennett, A. L. B. Pyne, and R. A. McKendry, "Cantilever sensors for rapid optical antimicrobial sensitivity testing," *ACS Sens.* **5**(10), 3133–3139 (2020).
25. A. Mustazzolu, L. Venturelli, S. Dinarelli, K. Brown, R. A. Floto, G. Dietler, L. Fattorini, S. Kasas, M. Girasole, and G. Longo, "A rapid unraveling of the activity and antibiotic susceptibility of mycobacteria," *Antimicrob. Agents Chemother.* **63**(3), e02194 (2019).
26. S. Kasas, F. S. Ruggeri, C. Benadiba, C. Maillard, P. Stupar, H. Tournu, G. Dietler, and G. Longo, "Detecting nanoscale vibrations as signature of life," *Proc. Natl. Acad. Sci. U.S.A.* **112**(2), 378–381 (2015).
27. M. I. Vallalba, P. Stupar, W. Chomicki, M. Bertacchi, G. Dietler, L. Arnal, M. E. Vela, O. Yantorno, and S. Kasas, "Nanomotio detection method for testing antibiotic resistance and susceptibility of slow-growing bacteria," *Small* **14**(4), 1702671 (2018).
28. P. Stupar, O. Oputa, G. Longo, G. Prod'Hom, G. Dietler, G. Greub, and S. Kasas, "Nanomechanical sensor applied to blood culture pellets: a fast approach to determine the antibiotic susceptibility against agents of bloodstream infections," *Clin. Microbiol. Infect.* **23**(6), 400–405 (2017).
29. F. Pujol-Vila, R. Villa, and M. Alvarez, "Nanomechanical sensors as a tool for bacteria detection and antibiotic susceptibility testing," *Front. Mech. Eng.* **6**, 44 (2020).
30. H. Etayash, M. F. Khan, K. Kaur, and T. Thundat, "Microfluidic cantilever detects bacteria and measures their susceptibility to antibiotics in small confined volumes," *Nat. Commun.* **7**(1), 12947 (2016).
31. C. Xiong, J. T. Zhou, C. R. Liao, M. Zhu, Y. Wang, S. Liu, C. Li, Y. F. Zhang, Y. Y. Zhao, Z. S. Gan, L. Venturelli, S. Kasas, X. M. Zhang, G. Dietler, and Y. P. Wang, "Fiber-tip polymer microcantilever for fast and highly sensitive hydrogen measurement," *ACS Appl. Mater. Interfaces* **12**(29), 33163–33172 (2020).

32. H. Hillmer, C. Woidt, A. Kobylinskiy, M. Kraus, A. Istock, M. S. Q. Iskandar, R. Brunner, and T. Kusserow, "Miniaturized interferometric sensors with spectral tunability for optical fiber technology-a comparison of size requirements, performance, and new concepts," *Photonics* **8**(8), 332 (2021).
33. J. Ma, "Miniature fiber-tip Fabry-Perot interferometric sensors for pressure and acoustic detection," Ph.D. dissertation (The Hong Kong Polytechnic University, 2014).
34. S. Wu, Z. Zhang, X. Zhou, H. Liu, C. Xue, G. Zhao, Y. Cao, Q. Zhang, and X. Wu, "Nanomechanical sensors for direct and rapid characterization of sperm motility based on nanoscale vibrations," *Nanoscale* **9**(46), 18258–18267 (2017).